J Shoulder Elbow Surg (2019) 28, 570–577

ELSEVIER

Journal of Shoulder and Elbow Surgery

www.elsevier.com/locate/ymse

Influence of humeral abduction angle on axial rotation and contact area at the glenohumeral joint

Wataru Sahara, MD, PhD[a,*], Takaharu Yamazaki, PhD[b], Shoji Konda, PhD[c], Kazuomi Sugamoto, MD, PhD[d], Hideki Yoshikawa, MD, PhD[a]

[a]*Department of Orthopaedic Surgery, Osaka University Graduate School of Medicine, Suita, Japan*
[b]*Department of Information Systems, Saitama Institute of Technology, Fukaya, Saitama, Japan*
[c]*Department of Health and Sport Sciences, Osaka University Graduate School of Medicine, Suita, Japan*
[d]*Department of Orthropaedic Biomaterial Science, Osaka University Graduate School of Medicine, Suita, Japan*

Background: Although the elevation angle of the arm affects the range of rotation, it has not been evaluated up to the maximal abduction angle. In this study we conducted an evaluation up to maximal abduction and determined the contact patterns at the glenohumeral (GH) joint.
Methods: Fourteen healthy volunteers (12 men and 2 women; mean age, 26.9 years) with normal shoulders (14 right and 8 left) were instructed to rotate their shoulders at 0°, 90°, 135°, and maximal abduction for each shoulder at a time. Using 2-dimensional and 3-dimensional single-plane image registration, the internal rotation (IR), external rotation (ER), and range of motion (ROM; ie, axial rotations) at the thoracohumeral (TH) and GH joints, and the contribution ratio (%ROM = GH-ROM/TH-ROM) were calculated for each abduction. The glenoid position with respect to the humeral head was also analyzed.
Results: The TH-IR and TH-ER shifted toward an ER with increasing abduction angle, whereas the TH-ROM significantly decreased except at abduction between 0° and 90° ($P < .001$). The GH-IR and GH-ROM significantly decreased except at abduction between 0° and 90° ($P < .001$), but the GH-ER remained constant regardless of the abduction. The contribution ratio exceeded 80% for every abduction angle. The glenoid moved on the central and posterior areas of the humeral head at 0° and 90° abduction, respectively, and on the posterosuperior and anterosuperior areas at 135° and maximal abduction, respectively.
Conclusion: Our results provide new knowledge about wide axial rotation up to maximal abduction and constant GH-ER at any abduction.
Level of evidence: Basic Science; Kinesiology

Keywords: Shoulder kinematics; 2D/3D image registration; axial rotation; abduction; glenohumeral rotation; contact area

The combination of elevation and axial rotation of the upper limb enables the performance of various activities of daily living and sports practice. Other studies have addressed the relationship between axial rotation of the arm and activities of daily living.[3,15,24,26,35,36] Specifically, an external rotation (ER)

The Osaka University Academic Clinical Research Center Institutional Review Board approved this study (ID no. 10189).

*Reprint requests: Wataru Sahara, MD, PhD, Department of Orthopaedic Surgery, Osaka University Graduate School of Medicine, 2-2 Yamada-oka, Suita 565-0871, Japan.
E-mail address: w-sahara@umin.ac.jp (W. Sahara).

1058-2746/$ - see front matter
https://doi.org/10.1016/j.jse.2018.08.023

with approximately 90° abduction can represent tasks such as combing hair and reaching overhead, whereas internal rotation (IR) can represent abdominal and perineal care. This assessment is important for the functional evaluation of the shoulder in patients with postoperative rotator cuff repair and arthroplasty and can be considered as a goal of rehabilitation in the range of motion (ROM) to recover the ability to perform activities of daily living.

Likewise, an axial rotation at high abduction can represent overhead motions in throwing and racket-based sports.[1,11,12,20,29] In 1934, Codman[2] claimed that the ROM of the humerus diminishes with its elevation and that it can neither rotate externally nor internally at complete elevation. Then, Saha[27] reported that the glenohumeral (GH) joint losses active rotation when the humeral shaft is aligned with the scapular spine, which is a condition called the zero position. Although the GH joint is close to the zero position during ball release in a throwing motion, it preserves some range of axial rotation, thus contradicting Saha's statement.[12,21]

Recent in vivo studies suggest that the elevation angle and plane of the arm influence the range of rotation,[4,6,7] but there is no such evaluation up to maximal abduction. Although numeric character data about the thoracohumeral (TH) and GH rotations have been provided in reports using electromagnetic tracking devices, evaluations such as the contact pattern of the GH joint and relative position between the glenoid and the insertion of rotator cuff muscles have not been addressed. This study evaluated the influence of the abduction angle on the range of axial rotation up to maximal abducted rotation and contact patterns at the GH joint.

Materials and methods

Participants

The study enrolled 14 healthy volunteers (12 men and 2 women) without shoulder complaints, including pain and restricted motion or any previous history of shoulder surgery or traumatic injury. The participants were a mean age 26.9 ± 5.9 years (range, 24-39 years), and their mean height and weight were 170.1 ± 8.0 cm, and 61.6 ± 8.2 kg, respectively. The participants provided informed consent.

Image acquisition

High-resolution computed tomography (CT) scans were acquired from both shoulders of each participant using the Aquilion 64 CT scanner (Toshiba Medical Systems Co., Ltd., Tochigi, Japan). Sequential axial images of 0.5-mm thickness with a resolution of 512 × 512 pixels were obtained from the clavicle to the distal humerus, and the corresponding Digital Imaging and Communications in Medicine (National Electrical Manufacturers Association, Rosslyn, VA, USA) data were transferred to a 3-dimensional (3D) image analysis system (Volume Analyzer, Synapse Vincent 3; Fujifilm Medical Co., Ltd., Tokyo, Japan). The clavicle, scapula, humerus, and ribs were automatically segmented, and 3D bone models were created from the segmented area that exceeded 80 to 120 Hounsfield units.

Figure 1 Image acquisition using fluoroscopy. The participant in the photograph was asked to rotate externally his arm at 90° abduction. The intensifier was tilted 25° in the craniocaudal direction to reduce overlapping between the scapula and ribs and increase overlapping between the humeral head and glenoid.

Dynamic fluoroscopic images from 22 shoulders (14 right and 8 left shoulders) were obtained using a single-plane fluoroscopy system with 17-inch image intensifiers (C-vision Safire 17; Shimadzu Corp., Kyoto, Japan). The image included data from the first to the fourth rib, the whole clavicle and scapula, and the proximal half of the humerus. Images were recorded as 7.5-Hz serial spot images with a resolution of 1024 × 1024 pixels. The volunteers stood between an examination table and a C-arm, which was tilted 25° in the craniocaudal direction (not anteroposterior direction conforming to the true anteroposterior view of x-ray) as shown in Fig. 1. This direction was selected to reduce overlapping between the scapula and ribs while increasing the overlap between the humeral head and glenoid.

The participants were instructed to hold their breath to prevent rib motions while performing active maximal IRs and ERs at 0°, 90°, 135°, and maximal abduction in the coronal plane with the elbow flexed. The examiner measured the abduction angle using a goniometer while holding the subject's elbow to keep the abduction angle. The starting position, denoted as neutral rotation (NR), was set with the forearm pointing forward for the 0° and 90° abductions and parallel to the coronal plane for the 135° and maximal abductions. The study subjects rotated their arms following the sequence NR, ER, NR, IR, and NR. The movement consisted of 3 seconds of rotation, followed by 1 second of pause between rotations.

Image registration

Three fluoroscopic images at ER, NR, and IR were selected for analysis. The original images were transformed into line drawings. However, the contours of the scapula, clavicle, and first to fourth ribs were overlapped and thus difficult to determine. Each bone model

was therefore manually superimposed on the original images, and rough contours with a 2-pixel width were automatically determined for each bone based on the superimposed model. These rough contours were then manually processed to remove noise.

To estimate the 3D orientation of the bone models, the root-mean-square distance between the bone model and line drawing of each image contour (ie, 2D/3D shape matching registration) was minimized using the Motion Analysis software, which was developed at our laboratory.[39] The error in the direction perpendicular to the image plane during single-plane image registration was corrected as follows. The distances between the sternoclavicular, acromioclavicular, and GH joints were estimated using the orientation of the bone models from the CT scans. First, the orientation of the clavicle was corrected in the direction perpendicular to the image plane by adapting the same distance to the acromioclavicular joint at the image registration. Then, the orientation of the sternum and first to fourth ribs was corrected by adapting that of the sternoclavicular joint, whereas the orientation of the humerus was corrected by adapting that of the GH joint.

Motion analysis

The local coordinate systems of the thorax (sternum and first to fourth ribs), scapula, and humerus were defined according to the definition proposed by the International Society of Biomechanics.[37] Specifically, the origin of the thorax (O_t) coordinate system was located at the center of mass of the sternum manubrium (Fig. 2, *A*). In addition, the X_t–Y_t plane was set to be the plane including the long axis of the sternum, and the Y_t axis was colinear to the spinous process of the fourth thoracic vertebra and the origin. The origin of the scapula (O_s) coordinate system was the centroid of the glenoid, with the Z_s axis perpendicular to the glenoid fossa, and the X_s and Y_s axes corresponded to the inferosuperior and anteroposterior direction of the glenoid, respectively (Fig. 2, *B*). Finally, the origin of the humerus (O_h) coordinate system was the center of the sphere fitting the humeral head, the X_h axis was parallel to the humeral shaft, the Y_h axis was perpendicular to the line connecting the lateral and medial epicondyle, and the Z_h axis corresponded to the lateromedial direction (Fig. 2, *C*).

The 3D orientations of the humerus with respect to the thorax and scapula (ie, TH and GH joints) during ER and IR were expressed using Cardan angles as recommended by Bonnefoy-Mazure et al[1] to prevent gimbal lock.[19,31] The humerus motion sequences were rotations around the Y_h (+, adduction; –, abduction), Z_h (+, flexion; –, extension), and X_h (+, ER; –, IR) axes (Fig. 2, *C*).

For motion analysis, the axial rotations of the TH and GH joints during ER and IR were calculated. Likewise, the total ROM (ie, axial rotation) at the TH and GH joints was calculated as the ROM difference between the ER and IR, and the contribution ratio (%ROM) was calculated as GH-ROM/TH-ROM.

Finally, the anteroposterior and superoinferior position of the glenoid center with respect to the humeral head was expressed as longitude and latitude by representing the humeral head as a globe. The intersection between the articular surface of the humeral head and the perpendicular line to the anatomic neck plane of the humerus through the center of the humeral head was defined as 0° of longitude and latitude (Fig. 3, *A*). Positive values of longitude and latitude indicate the anterior and superior parts of the humeral head, respectively. The inclination of the long axis of the glenoid was expressed as the angle between the longitudinal line of the humeral head and the long axis of the glenoid thus being 0° when the longitudinal line and long axis are parallel. Likewise, the positive and negative values indicate inclination of the superior pole of the glenoid toward the lesser and greater tuberosities of the humerus, respectively.

Validation procedure

The accuracy of the evaluation system was calculated by applying total knee arthroplasty with reported in-plane and out-of-plane translations of 0.2 to 0.4 mm and 1.5 mm, respectively, and in-plane and out-of-plane rotations of 0.3° and 0.7° to 0.9°, respectively.[39] In the

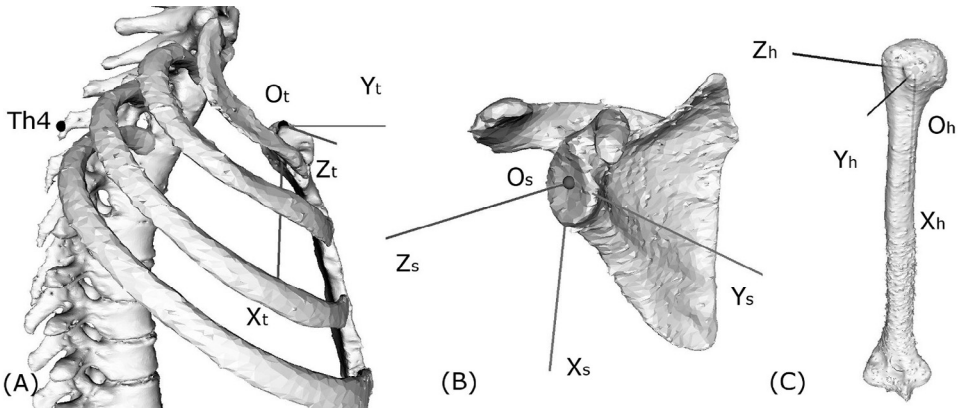

Figure 2 Definition of the local coordinate systems (LCS). (**A**) The origin (O_t) of the thorax LCS is located at the center of mass of the sternum manubrium. The X_t–Y_t plane is set to be the plane including the long axis of the sternum, and the Y_t axis is colinear to the spinous process of the fourth thoracic vertebra and the origin. (**B**) The origin (O_s) of the scapula LCS is the centroid of the glenoid, with the Z_s axis perpendicular to the glenoid fossa, and the X_s and Y_s axes correspond to the inferosuperior and anteroposterior direction of the glenoid, respectively. (**C**) The origin of the humerus (O_h) LCS is the center of the sphere fitting the humeral head, the X_h axis is parallel to the humeral shaft, the Y_h axis is perpendicular to the line connecting the lateral and medial epicondyle, and the Z_h axis is the lateromedial direction. The sequence of humeral motions correspond to rotations around the Y_h (+, adduction; –, abduction), Z_h (+, flexion; –, extension), and X_h (+, external; –, internal rotation) axes.

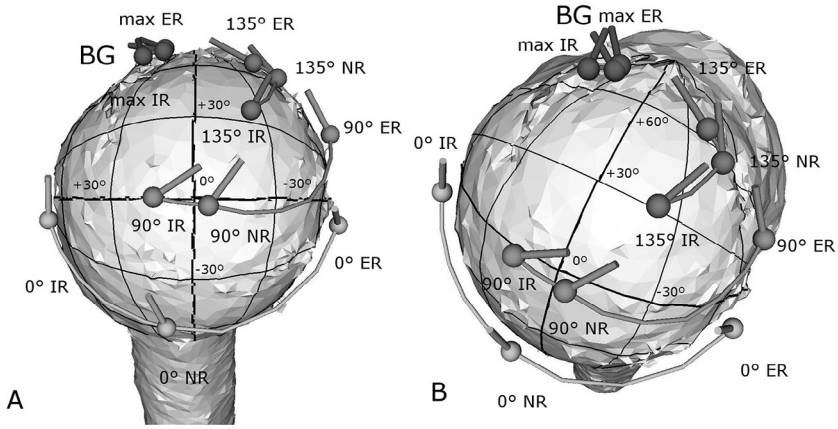

Figure 3 Glenoid movement on the humeral head. The graphs show the glenoid positions of the right shoulder at external (*ER*), neutral (*NR*), and internal rotations (*IR*) for abduction angles 0°, 90°, 135°, and maximal abduction (*max*). The humeral head shown in (**A**) superomedial and (**B**) posterosuperior views. The *spheres* represent the glenoid center, and the *short bars* are the superior directions of the glenoid, which are parallel to the X_s axis (Fig. 2, *B*). The glenoid motion is wide on the humeral head at 0° and 90° abduction, but limited at 135° and maximal abduction. *BG*, bicipital groove.

present study, 2 validation studies were performed to confirm the accuracy for in vivo shoulder bone models. First, the orientation of the clavicle, scapula, and humerus with respect to the ribs was calculated using the Multipurpose Chest Phantom N1 "Lungman" (Kyoto Kagaku Co., Ltd., Kyoto, Japan), which is applicable to plane radiography and CT scanning. The phantom precisely imitates the upper half of the human body, including lung, trachea, ribs, clavicle, scapula, humerus, and surrounding soft tissues at an elevated position of the upper limb. We obtained fluoroscopic and CT images from the phantom and calculated the difference between the 3D orientation of the clavicle, scapula, and humerus with respect to the thorax retrieved from the 2D/3D image registration and from the CT scanning. The translational and rotational differences were, respectively, 0.7 to 1.9 mm and 0.3° to 1.6° for the clavicle, 0.7 to 1.2 mm and 1.0° to 1.4° for the scapula, and 0.8 to 1.4 mm and 0.7° to 1.1° for the humerus.

Second, the GH joint orientation was calculated using humeral and scapular imitation bones (Medical Imaging Phantoms; Kyoto Kagaku Co., Ltd.). Specifically, Styrofoam (Dow Chemical Company, Midland, MI, USA) was placed between the humeral head and the glenoid of the phantoms for imitating the joint space. These phantoms were fixed at 6 positions using a variable grasper, and then CT and fluoroscopic images were obtained at each position. The differences of GH orientation between the 2D/3D registration and CT images were calculated in terms of root-mean-square errors. The in-plane and out-of-plane translations were 0.4 to 0.7 mm and 1.1 mm, respectively, and in-plane and out-of-plane rotations were 1.1° and 3.0° to 3.8°, respectively.

Statistical analysis

To compare both the axial rotations and ROM at the TH and GH joints for different abduction angles, 2-way repeated analysis of variance, followed by a post hoc Tukey test, were performed with 2 within-subject factors (abduction angle and axial rotation). The statistical analysis was performed using JMP Pro 12 software (SAS Institute Inc., Cary, NC, USA), with the level of significance at $P < .05$.

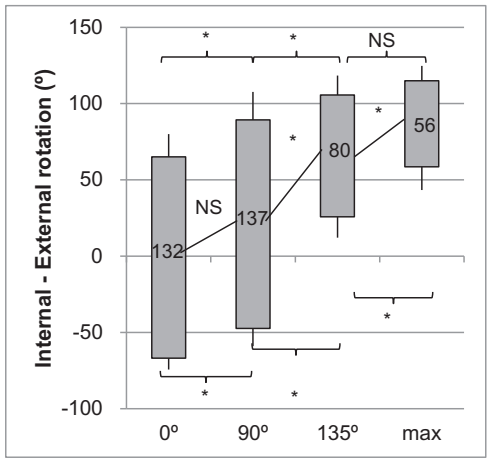

Figure 4 Mean and standard deviation of the thoracohumeral (TH) axial rotation during external rotation (TH-ER) and internal rotation (TH-IR) for every abduction angle. The values in the boxes indicate the range of axial rotation (TH-ROM). The TH-ER and TH-IR shifted toward external rotation, whereas the TH-ROM decreased with increasing abduction angle. *$P < .01$. *NS*, not significant; *max*, maximal abduction.

Results

TH rotation

The abduction angles of the humerus relative to the thorax were 2.0° ± 3.4° at 0°, 87.5° ± 4.6° at 90°, 131.3° ± 8.1° at 135°, and 161.4° ± 8.0° at maximal abduction (Fig. 4 and Table I). The TH axial rotations during ER (TH-ER) shifted toward ER as the abduction angle increased: 65.1° ± 14.9° at 0°, 89.3° ± 18.3° at 90°, 105.7° ± 12.7° at 135°, and 115.0° ± 9.8° at maximal abduction. There were significant differences among the abductions, except between 135° and maximal abduction ($P < .01$). The TH axial rotations during

Table I Mean and standard deviation of thoracohumeral and glenohumeral axial rotations and range of motion during external and internal rotation at every abduction angle

Variable	ER, °	*P* value*	IR, °	*P* value	ROM, °	*P* value*
TH axial rotation						
0°	65.1 ± 14.9	<.0001	−66.9 ± 7.4	<.0001	132.0 ± 17.2	.8656
90°	89.3 ± 18.3	.002	−47.4 ± 11.6	<.0001	136.7 ± 23.8	<.0001
135°	105.7 ± 12.7	.4452	25.8 ± 13.7	<.0001	80.0 ± 22.8	<.0001
Maximum	115.0 ± 9.8		58.6 ± 15.2		56.4 ± 16.3	
GH axial rotation						
0°	96.7 ± 12.3	.0656	−16.6 ± 6.7	.9433	113.3 ± 13.9	.6076
90°	107.0 ± 15.1	.0866	−12.0 ± 7.8	<.0001	119.0 ± 15.2	<.0001
135°	97.2 ± 11.6	.9511	24.2 ± 12.2	<.0001	73.0 ± 18.7	<.0001
Maximum	92.5 ± 7.6		45.8 ± 11.1		46.6 ± 13.0	

ER, external rotation; *IR*, internal rotation; *ROM*, range of motion; *TH*, thoracohumeral; *GH*, glenohumeral motion.
* The *P* value indicates the comparison at a given axial rotation with abduction angles between adjacent rows.

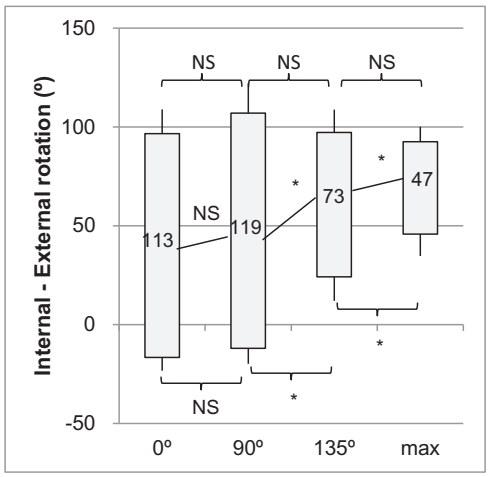

Figure 5 Mean and standard deviation of the glenohumeral (GH) axial rotation during external rotation (GH-ER) and internal rotation (GH-IR) for every abduction angle. The values in the boxes indicate the range of axial rotation (GH-ROM). The GH-ER remained constant, whereas the GH-IR and GH-ROM decreased with the increasing abduction angle. **P* < .01. *NS*, not significant; *max*, maximal abduction.

IR (TH-IR) also shifted toward ER as the abduction angle increased: −66.9° ± 7.4° at 0°, −47.4° ± 11.6° at 90°, 25.8° ± 13.7° at 135°, and 58.6° ± 15.2° at maximal abduction. There were significant differences among all of the abductions ($P < .0001$). The ROM for axial rotation (TH-ROM) significantly decreased except at 0° and 90° abduction (132° ± 17.2° at 0°, 136.7° ± 23.8° at 90°, 80.0° ± 22.8° at 135°, and 56.4° ± 16.3° at maximal abduction; $P < .0001$).

GH rotation

The abduction angles of the humerus relative to the scapula were 6.2° ± 8.3° at 0°, 48.2° ± 6.1° at 90°, 81.9° ± 6.7° at 135°, and 103.3° ± 8.3° at maximal abduction (Fig. 5 and Table I). The GH axial rotations during ER (GH-ER) remained constant for all the abductions (96.7° ± 12.3° at 0°, 107° ± 15.1° at 90°, 97.2° ± 11.6° at 135°, and 92.5° ± 7.6° at maximal abduction; $P > .05$). The GH axial rotations during IR (GH-IR) shifted toward ER as the abduction angle increased: −16.6° ± 6.7° at 0°, −12.0° ± 7.8° at 90°, 24.2° ± 12.2° at 135°, and 45.8° ± 11.1° at maximal abduction. There were significant differences among the abductions, except between 0° and 90° abduction ($P < .0001$). The ROM for axial rotation (GH-ROM) significantly decreased except at 0° and 90° abduction (113.3° ± 13.9 at 0°, 119° ± 15.2° at 90°, 73.0° ± 18.7° at 135°, and 46.6° ± 13.0° at maximal abduction; $P < .0001$).

The contribution ratios (%ROM) of the GH joint were 86.0% ± 4.8% at 0°, 87.8% ± 6.4% at 90°, 92.1% ± 4.9% at 135°, and 83.2% ± 7.7% at maximal abduction. Therefore, the GH joint was the main contributor to axial rotation.

Glenoid movement on the humeral head

At 0° abduction, the glenoid moved evenly from the anterior to posterior positions of the humeral head (Fig. 3 and Table II) with a slightly inferior level, and its inclination ranged from –9.9° ± 13.6° (IR) to 36.3° ± 10.8° (ER). At 90° abduction, it moved more toward the posterior area of the humeral head with central level (latitude was close to 0°), and its inclination increased in the range from –52.9° ± 7.1° (IR) to 55.8° ± 19.9° (ER). In addition, at 135° and maximal abductions, it was localized on the posterosuperior and anterosuperior area of the humeral head, respectively. Although the glenoid moved widely on the humeral head during axial rotation at 0° and 90° abduction, its inclination reduced as the abduction angle increased, ranging from –15.4° ± 17.5° (IR) to 59.0° ± 11.9° (ER) at 135° abduction and from 7.0° ± 15.6° (IR) to 54.6° ± 8.6° (ER) at maximal abduction.

Discussion

The range of axial rotation of the GH joint is important for clinically assessing shoulder function. For instance, some

Table II Glenoid motion on the humeral head*

Variable	ER, °	*P* value†	IR, °	*P* value†
Longitude				
0°	−54.9 ± 11.1	.8094	56.3 ± 9.2	<.0001
90°	−48.9 ± 20	<.0001	16.3 ± 9.5	<.0001
135°	−15.7 ± 8.8	<.0001	−8.7 ± 9.6	<.0001
Maximum	7.6 ± 8.1		7.7 ± 7.7	
Latitude				
0°	−31.3 ± 12.8	<.0001	−6.0 ± 13.1	.9433
90°	33.9 ± 24.3	<.0001	−1.4 ± 6.9	<.0001
135°	49.8 ± 6.1	1	32.6 ± 9.7	<.0001
Maximum	50.3 ± 6.2		51.9 ± 9.1	
Inclination				
0°	36.3 ± 10.8	.0002	−9.9 ± 13.6	<.0001
90°	55.8 ± 19.9	.9996	−52.9 ± 7.1	<.0001
135°	59.0 ± 11.9	.9929	−15.4 ± 17.5	<.0001
Maximum	54.6 ± 8.6		7.0 ± 15.6	

* The position of the glenoid center is expressed as longitude and latitude by representing the humeral head as a globe. The positive values of longitude and latitude indicate the anterior and superior part of the humeral head, respectively. The inclination is expressed as the angle between the longitudinal line of the humeral head and the long axis of the glenoid. The positive and negative values indicate inclination of the superior pole of the glenoid towards the lesser and greater tuberosities of the humerus, respectively.

† *P* value indicates the comparison at a given axial rotation with abduction angles between adjacent rows.

athletes of throwing sports exhibit increased ER and decreased IR,[14] and measuring axial rotation at 0° and 90° abduction is often used to evaluate injured or postoperative conditions. Rundquist et al[25] and McCully et al[18] used 3D electromagnetic tracking to evaluate TH rotations of normal subjects during axial rotation at 0° and 90° abduction. Their results showed that TH-ER increases and TH-IR decreases with increasing abduction angle, which were similar to the results reported in the present study, but we also found that their TH-ER at 0° and 90° abduction tended to reduce according to the subject's age. Moreover, Humphries et al[6] evaluated GH rotations of subjects with normal shoulders during axial rotation at 60°, 90°, and 120° abduction. Consistent with the results from the present study, they reported a constant GH-ER and decreasing GH-IR and GH-ROM with increasing abduction angle.

The axial rotation at maximal abduction is the most important contribution of the present study. As mentioned above, Codman[2] and Saha[27] claimed that axial rotation of the humerus was locked and diminished at maximal elevation, whereas Southgate et al[30] measured the range of axial rotation at 30°, 60°, and 90° abduction in a study using cadaveric specimens and reported respective ranges of 140°, 134°, and 93°. Likewise, the present study revealed that in vivo TH and GH rotations at approximately 50° and 40° of rotation, respectively, still enable large rotations at maximal abduction.

The contribution of scapular rotations during axial rotation could be estimated from the contribution ratio of the GH rotation to TH rotation. If the axial rotation had approached 0° at maximal elevation, as reported by Codman[2] and Saha,[27] the ratio would have decreased for increasing abduction. However, the present study showed it remained above 80% over any abduction angle, indicating that the scapula contribution is almost negligible during the axial rotation of the arm. These results are consistent with those reported in previous studies.[10,17,23,25] In fact, McClure et al[17] reported that the scapula does not rotate during IR and ER, except at maximal ER, when it also shows upward rotation, retraction, and posterior tilting. These findings suggest that the scapula serves as the foundation of the shoulder girdle during axial rotation at every abduction.

Most studies have addressed humeral motion with respect to the glenoid to evaluate the GH motion. However, this motion is difficult to understand because the humerus exhibits wide and complex motion in 3D space. In the present study, the glenoid motion with respect to the humeral head can additionally indicate characteristics such as the change of the contact area at the GH joint and the position relationship between the glenoid and the insertion of rotator cuff muscles. This approach was applied in our previous study to evaluate abduction.[28] Furthermore, the results from the present study are similar to those reported by Inui et al[7] during axial rotation at 45°, 90°, and 135° scapular abduction using 3D magnetic resonance imaging. The results on glenoid motion can explain the constant GH-ER at any abduction, but such conclusion cannot be drawn from cadaveric studies on soft tissue restrictors, such as the superior, middle, and anterior band of inferior glenohumeral ligaments, and the subscapularis tendon, which were reported to act as a restrictor for GH-ER at different GH abductions.[8,33,34] Moreover, the present study determined long axes of the glenoid located parallel to the edge of the rotator cuff insertion at 90°, 135°, and maximal abduction with ER (Fig. 3,

B and Supplementary Video). Thus, the posterior edge of the glenoid was close to the edge of the rotator cuff insertion, and the glenoid might be restricted by the insertion at ER.

The knowledge of the contact between the glenoid and humeral head during motion may provide clinically useful information. For instance, Yamamoto et al[38] evaluated the orientation of the glenoid on the humeral head using an approach called glenoid track. The approach was evaluated during maximal ER at different abduction degrees in cadaveric specimens to determine the size of a Hill-Sachs lesion that requires treatment, aimed for patients with anterior instability of the shoulder. Subsequently, Omori et al[22] used glenoid track to evaluate in vivo subjects. Furthermore, this approach might be used to resemble GH motion during throwing motion. Konda et al[12] reported a GH elevation reaching approximately 87° and the humerus almost aligned with the scapular spine in the late cocking phase. This phase corresponds to GH elevation between 135° and maximal abduction in the present study. Comparing the glenoid motion during axial rotation below and above 90° abduction, a limited range of the humeral head motion occurred above 135° abduction. In addition, Takagi et al[32] reported that the larger horizontal abduction angle induced anterior force at the GH joint. Hence, rotation of the humeral shaft aligned with the scapular spine may help to prevent shoulder disorders caused by the execution of throwing motions, because it reduces the load to the GH joint.

Overall, the present study provides different contributions such as the reported tracking of ribs by 2D/3D registration, evaluation of TH and GH rotation at high abduction on standing position under the action of gravity, and visualization of joint motion using 3D bone models. In addition, 3D electromagnetic tracking devices, which provide real-time motion processing, have allowed us to determine that the measurement error of the scapular orientation increases above 120° of elevation and that of the humeral rotation reaches 30° during axial rotation of the arm.[5,9] Although 3D CT accurately provides the location and morphology of the GH joint, it has drawbacks, including imaging restricted to the supine position and radiation exposure. Likewise, 3D magnetic resonance imaging, which accurately locates the GH joint using volume registration technique,[28] is not suitable to evaluate 3D orientation of the ribs given its limited field of view. In contrast, 2D/3D registration overcomes these drawbacks, and biplane registration has been reported to have higher measurement accuracy than single-plane registration.[13,16] Nevertheless, biplane registration may be inadequate for motion analysis beyond 135° of abduction with axial rotation due to obstruction by the neck and mandible during image acquisition.

The present study has some limitations, such as the small number and young age of the participants. For instance, Rundquist et al[25] evaluated individuals who were approximately 51 years old and reported smaller TH-ER and GH-ER than those of the present study. Consequently, the results of the present study cannot be applied for older subjects, and future studies should consider more subjects and diversity. In addition, because the IR at 0° of abduction was obstructed by the abdomen, it was not maximal.

Conclusion

We evaluated the influence of the abduction angle on the range of axial rotation and contact pattern at the GH joint during axial rotation up to maximal abduction. The TH-IR and TH-ER shifted toward ER with increasing abduction angle, and the TH-ROM decreased except between 0° and 90° abduction. In addition, the GH-IR and GH-ROM significantly decreased with the abduction angle, except between 0° and 90°, and the GH-ER remained constant. The glenoid moved widely on the humeral head at 0° and 90° abduction but moved on a limited area of the humeral head at 135° and maximal abduction.

Disclaimer

Wataru Sahara has received funding from Japan Society for the Promotion of Science (JSPS) Grant-in-Aid for Scientific Research (KAKENHI) grant no. JP26462241.

Kazuomi Sugamoto holds the majority of shares of teamLabBody. The other authors, their immediate families, and any research foundation with which they are affiliated have not received any financial payments or other benefits from any commercial entity related to the subject of this article.

Supplementary data

Supplementary data to this article can be found online at https://doi.org/10.1016/j.jse.2018.08.023.

References

1. Bonnefoy-Mazure A, Slawinski J, Riquet A, Leveque JM, Miller C, Cheze L. Rotation sequence is an important factor in shoulder kinematics. Application to the elite players' flat serves. J Biomech 2010;43:2022-5. http://dx.doi.org/10.1016/j.jbiomech.2010.03.028
2. Codman EA. Chapter 2: normal motions of the shoulder joint. In: Codman EA, editor. The shoulder: rupture of the supraspinatus tendon and other lesions in or about the subacromial bursa. New York: G. Miller & Co. Medical Publishers, Inc.; 1984. p. 32-64 ISBN: 0-89874-731-7.
3. Gates DH, Walters LS, Cowley J, Wilken JM, Resnik L. Range of motion requirements for upper-limb activities of daily living. Am J Occup Ther 2016;70:7001350010p1-10. http://dx.doi.org/10.5014/ajot.2016.015487
4. Haering D, Raison M, Begon M. Measurement and description of three-dimensional shoulder range of motion with degrees of freedom interactions. J Biomech Eng 2014;136:084502. http://dx.doi.org/10.1115/1.4027665
5. Hamming D, Braman JP, Phadke V, LaPrade RF, Ludewig PM. The accuracy of measuring glenohumeral motion with a surface humeral cuff.

J Biomech 2012;45:1161-8. http://dx.doi.org/10.1016/j.jbiomech.2012.02.003
6. Humphries A, Cirovic S, Bull AM, Hearnden A, Shaheen AF. Assessment of the glenohumeral joint's active and passive axial rotational range. J Shoulder Elbow Surg 2015;24:1974-81. http://dx.doi.org/10.1016/j.jse.2015.07.007
7. Inui H, Tanaka H, Nobuhara K. Glenohumeral relationships at different angles of abduction. Surg Radiol Anat 2014;36:1009-14. http://dx.doi.org/10.1007/s00276-014-1315-5
8. Jansen JH, de Gast A, Snijders CJ. Glenohumeral elevation-dependent influence of anterior glenohumeral capsular lesions on passive axial humeral rotation. J Biomech 2006;39:1702-7. http://dx.doi.org/10.1016/j.jbiomech.2005.04.022
9. Karduna AR, McClure PW, Michener LA, Sennett B. Dynamic measurements of three-dimensional scapular kinematics: a validation study. J Biomech Eng 2001;123:184-90.
10. Koishi H, Goto A, Tanaka M, Omori Y, Futai K, Yoshikawa H, et al. In vivo three-dimensional motion analysis of the shoulder joint during internal and external rotation. Int Orthop 2011;35:1503-9. http://dx.doi.org/10.1007/s00264-011-1219-5
11. Konda S, Yanai T, Sakurai S. Scapular rotation to attain the peak shoulder external rotation in tennis serve. Med Sci Sports Exerc 2010;42:1745-53. http://dx.doi.org/10.1249/MSS.0b013e3181d64103
12. Konda S, Yanai T, Sakurai S. Configuration of the shoulder complex during the arm-cocking phase in baseball pitching. Am J Sports Med 2015;43:2445-51. http://dx.doi.org/10.1177/0363546515594379
13. Kozono N, Okada T, Takeuchi N, Hamai S, Higaki H, Ikebe S, et al. In vivo kinematic analysis of the glenohumeral joint during dynamic full axial rotation and scapular plane full abduction in healthy shoulders. Knee Surg Sports Traumatol Arthrosc 2017;25:2032-40. http://dx.doi.org/10.1007/s00167-016-4263-2
14. Levine WN, Brandon ML, Stein BS, Gardner TR, Bigliani LU, Ahmad CS. Shoulder adaptive changes in youth baseball players. J Shoulder Elbow Surg 2006;15:562-6. http://dx.doi.org/10.1016/j.jse.2005.11.007
15. Magermans DJ, Chadwick EK, Veeger HE, van der Helm FC. Requirements for upper extremity motions during activities of daily living. Clin Biomech (Bristol, Avon) 2005;20:591-9. http://dx.doi.org/10.1016/j.clinbiomech.2005.02.006
16. Massimini DF, Boyer PJ, Papannagari R, Gill TJ, Warner JP, Li G. In-vivo glenohumeral translation and ligament elongation during abduction and abduction with internal and external rotation. J Orthop Surg Res 2012;7:29. http://dx.doi.org/10.1186/1749-799X-7-29
17. McClure PW, Michener LA, Sennett BJ, Karduna AR. Direct 3-dimensional measurement of scapular kinematics during dynamic movements in vivo. J Shoulder Elbow Surg 2001;10:269-77.
18. McCully SP, Kumar N, Lazarus MD, Karduna AR. Internal and external rotation of the shoulder: effects of plane, end-range determination, and scapular motion. J Shoulder Elbow Surg 2005;14:602-10. http://dx.doi.org/10.1016/j.jse.2005.05.003
19. Meskers CG, Vermeulen HM, de Groot JH, van Der Helm FC, Rozing PM. 3D shoulder position measurements using a six-degree-of-freedom electromagnetic tracking device. Clin Biomech (Bristol, Avon) 1998;13:280-92.
20. Miyashita K, Kobayashi H, Koshida S, Urabe Y. Glenohumeral, scapular, and thoracic angles at maximum shoulder external rotation in throwing. Am J Sports Med 2010;38:363-8. http://dx.doi.org/10.1177/0363546509347542
21. Nobuhara K. Chapter 9: the shoulder in sports. A: analysis of throwing motion and injuries. In: Nobuhara K, editor. The shoulder: its function and clinical aspects. Singapore: World Scientific Publishing Co. Pte. Ltd.; 2003. p. 401-37. ISBN: 978-4-260-01676-6
22. Omori Y, Yamamoto N, Koishi H, Futai K, Goto A, Sugamoto K, et al. Measurement of the glenoid track in vivo as investigated by 3-Dimensional motion analysis using open MRI. Am J Sports Med 2014;42:1290-5. http://dx.doi.org/10.1177/0363546514527406
23. Ribeiro A, Pascoal AG. Scapular contribution for the end-range of shoulder axial rotation in overhead athletes. J Sports Sci Med 2012;11:676-81.
24. Roren A, Lefevre-Colau MM, Roby-Brami A, Revel M, Fermanian J, Gautheron V, et al. Modified 3D scapular kinematic patterns for activities of daily living in painful shoulders with restricted mobility: a comparison with contralateral unaffected shoulders. J Biomech 2012;45:1305-11. http://dx.doi.org/10.1016/j.jbiomech.2012.01.027
25. Rundquist PJ, Anderson DD, Guanche CA, Ludewig PM. Shoulder kinematics in subjects with frozen shoulder. Arch Phys Med Rehabil 2003;84:1473-9. http://dx.doi.org/10.1016/S0003-9993(03)00359-9
26. Rundquist PJ, Obrecht C, Woodruff L. Three-dimensional shoulder kinematics to complete activities of daily living. Am J Phys Med Rehabil 2009;88:623-9. http://dx.doi.org/10.1097/PHM.0b013e3181ae0733
27. Saha AK. The classic mechanism of shoulder movements and a plea for the recognition of "zero position" of glenohumeral joint. Clin Orthop Relat Res 1983;(173):3-10.
28. Sahara W, Sugamoto K, Murai M, Tanaka H, Yoshikawa H. The three-dimensional motions of glenohumeral joint under semi-loaded condition during arm abduction using vertically open MRI. Clin Biomech (Bristol, Avon) 2007;22:304-12. http://dx.doi.org/10.1016/j.clinbiomech.2006.04.012
29. Seminati E, Marzari A, Vacondio O, Minetti AE. Shoulder 3D range of motion and humerus rotation in two volleyball spike techniques: injury prevention and performance. Sports Biomech 2015;14:216-31. http://dx.doi.org/10.1080/14763141.2015.1052747
30. Southgate DF, Hill AM, Alexander S, Wallace AL, Hansen UN, Bull AM. The range of axial rotation of the glenohumeral joint. J Biomech 2009;42:1307-12. http://dx.doi.org/10.1016/j.jbiomech.2009.03.007
31. Stokdijk M, Eilers PH, Nagels J, Rozing PM. External rotation in the glenohumeral joint during elevation of the arm. Clin Biomech (Bristol, Avon) 2003;18:296-302. http://dx.doi.org/10.1016/j.clinbiomech.2005.09.012
32. Takagi Y, Oi T, Tanaka H, Inui H, Fujioka H, Tanaka J, et al. Increased horizontal shoulder abduction is associated with an increase in shoulder joint load in baseball pitching. J Shoulder Elbow Surg 2014;23:1757-62. http://dx.doi.org/10.1016/j.jse.2014.03.005
33. Turkel SJ, Panio MW, Marshall JL, Girgis FG. Stabilizing mechanisms preventing anterior dislocation of the glenohumeral joint. J Bone Joint Surg Am 1981;63:1208-17.
34. Urayama M, Itoi E, Hatakeyama Y, Pradhan RL, Sato K. Function of the 3 portions of the inferior glenohumeral ligament: a cadaveric study. J Shoulder Elbow Surg 2001;10:589-94.
35. van Andel CJ, Wolterbeek N, Doorenbosch CA, Veeger DH, Harlaar J. Complete 3D kinematics of upper extremity functional tasks. Gait Posture 2008;27:120-7. http://dx.doi.org/10.1016/j.gaitpost.2007.03.002
36. Veeger HE, Magermans DJ, Nagels J, Chadwick EK, van der Helm FC. A kinematical analysis of the shoulder after arthroplasty during a hair combing task. Clin Biomech (Bristol, Avon) 2006;21(Suppl. 1):S39-44. http://dx.doi.org/10.1016/j.clinbiomech.2005.09.012
37. Wu G, van der Helm FC, Veeger HE, Makhsous M, Van Roy P, Anglin C, et al. ISB recommendation on definitions of joint coordinate systems of various joints for the reporting of human joint motion—part II: shoulder, elbow, wrist and hand. J Biomech 2005;38:981-92. http://dx.doi.org/10.1016/j.jbiomech.2004.05.042
38. Yamamoto N, Itoi E, Abe H, Minagawa H, Seki N, Shimada Y, et al. Contact between the glenoid and the humeral head in abduction, external rotation, and horizontal extension: a new concept of glenoid track. J Shoulder Elbow Surg 2007;16:649-56. http://dx.doi.org/10.1016/j.jse.2006.12.012
39. Yamazaki T, Watanabe T, Nakajima Y, Sugamoto K, Tomita T, Yoshikawa H, et al. Improvement of depth position in 2-D/3-D registration of knee implants using single-plane fluoroscopy. IEEE Trans Med Imaging 2004;23:602-12. http://dx.doi.org/10.1109/TMI.2004.826051